Structural Engineering and Mechanics, Vol. 25, No. 4 (2007) 405-421
DOI: http://dx.doi.org/10.12989/sem.2007.25.4.405

An assumed-stress hybrid element for static and free vibration analysis of folded plates

Kutlu Darılmaz†

Department of Civil Engineering, Istanbul Technical University 34469, Maslak, Istanbul, Turkey

(Received December 30, 2004, Accepted September 5, 2006)

Abstract. A four-node hybrid stress element for analysing orthotropic folded plate structures is presented. The formulation is based on Hellinger-Reissner variational principle. The element is developed by combining a hybrid plane stress element and a hybrid plate element. The proposed element has six degree of freedom per node and permits an easy connection to other type of elements. An equilibrated stress field in each element and inter element compatible boundary displacement field are assumed independently. Static and free vibration analyses of folded plates are carried out on numerical examples to show that the validity and efficiency of the present element.

Keywords: folded plate; assumed stress hybrid element; finite element; static analysis; free vibration.

1. Introduction

Folded-plate structures have been widely used in many fields such as folded-plate wall, silo, all kinds of containers, the auto industry, and shipbuilding. Therefore, there are real, practical needs for researching folded-plate structures. The FEM is the most powerful tool for the analysis of plates, in general, any continua. The folded plate structures can be solved by using flat shell elements which is a combination of membrane elements and plate elements. Many papers can be found in literature on folded plates which is based on this type of modelling. Perry *et al.* (1992) presented a rectangular hybrid element for analysing folded plates, Choi and Lee (1996) presented a variable-node flat shell element and solved some numerical examples also including folded plates, Eratli and Akoz (2002) formulated a functional and presented a rectangular element for folded plates with geometric and dynamic boundary conditions using Gateaux approach, Ayad and Rigolot (2002) presented a four-node hybrid mixed element based on mixed shear projected (MiSP) approach, Duan and Miyamoto (2002) proposed a family of shell elements of hybrid/mixed finite element method that accounts for transverse shear deformations based on a modified Hellinger-Reissner variational principle, Lee and Wooh (2004) deals with free vibration of folded structures and boxbeams made of composite materials using a four-noded Lagrangian and Hermite finite element that incorporates high order transverse shear deformation and rotary inertia.

In this paper, a flat shell element which is a combination of membrane element and a plate element is developed, based on the classical hybrid stress method which was first developed by Pian

† Associate Professor, E-mail: kdarilmaz@ins.itu.edu.tr

(1964). The element is generated by a combination of a hybrid plane stress element with drilling d.o.f. and a hybrid plate element presented by the author in a previous study, Darılmaz (2005). Static and free vibration analyses of folded plates are carried out to show the validity and efficiency of the present element.

2. Element stiffness formulation

The assumed-stress hybrid method is based on the independent prescriptions of stresses within the element and displacements on the element boundary. The element stiffness matrix is obtained using Hellinger-Reissner variational principle. The Hellinger-Reissner functional of linear elasticity allows displacements and stresses to be varied separately. This establishes the master fields. Two slave strain fields appear, one coming from displacements and one from stresses.

The Hellinger-Reissner functional can be written as

$$\Pi_{RH} = \int_V \{\sigma\}^T[D]\{u\}dV - \frac{1}{2}\int_V \{\sigma\}^T[S]\{\sigma\}dV \tag{1}$$

where $\{\sigma\}$ is the stress vector, $[S]$ is the compliance matrix relating strains, $\{\varepsilon\}$, to stress ($\{\varepsilon\} = [S]\{\sigma\}$), $[D]$ is the differential operator matrix corresponding to the linear strain-displacement relations ($\{\varepsilon\}=[D]\{u\}$) and V is the volume of structure.

The approximation for stresses and displacements can now be incorporated in the functional. The stress field is described in the interior of the element as

$$\{\sigma\} = [P]\{\beta\} \tag{2}$$

and a compatible displacement field is described by

$$\{u\} = [N]\{q\} \tag{3}$$

where $[P]$ and $[N]$ are matrices of stress and displacement interpolation functions, respectively, and $\{\beta\}$ and $\{q\}$ are the unknown stress and nodal displacement parameters, respectively. Intra-element equilibrating stresses and compatible displacements are independently interpolated. Since stresses are independent from element to element, the stress parameters are eliminated at the element level and a conventional stiffness matrix results. This leaves only the nodal displacement parameters to be assembled into the global system of equations.

Substituting the stress and displacement approximations Eq. (2), Eq. (3) in the functional Eq. (1) yields

$$\Pi_{RH} = [\beta]^T[G][q] - \frac{1}{2}[\beta]^T[H][\beta] \tag{4}$$

where

$$[H] = \int_V [P]^T[S][P]dV \tag{5}$$

$$[G] = \int [P]^T([D][N])dV \tag{6}$$

Now imposing stationary conditions on the functional with respect to the stress parameters $\{\beta\}$ gives

$$[\beta] = [H]^{-1}[G][q] \tag{7}$$

Substitution of $\{\beta\}$ in Eq. (4), the functional reduces to

$$\Pi_{RH} = \frac{1}{2}[q]^T[G]^T[H]^{-1}[G][q] = \frac{1}{2}[q]^T[K][q] \tag{8}$$

where

$$[K] = [G]^T[H]^{-1}[G] \tag{9}$$

is recognized as a stiffness matrix.

The solution of the system yields the unknown nodal displacements $\{q\}$. After $\{q\}$ is determined, element stresses or internal forces can be recovered by use of Eq. (7) and Eq. (2). Thus

$$\{\sigma\} = [P][H]^{-1}[G]\{q\} \tag{10}$$

3. Governing equations

Consider a folded plate of uniform thickness which the orthotropic material property may be arbitrarily oriented at an angle ϕ with refrence to the x-axis of the local coordinate system Fig. 1.

The stress-strain relation with respect to x, y and z axes can be written as

$$\begin{Bmatrix} \sigma_x \\ \sigma_y \\ \tau_{xy} \end{Bmatrix} = \begin{bmatrix} \bar{\Omega}_{11} & \bar{\Omega}_{12} & \bar{\Omega}_{16} \\ \bar{\Omega}_{12} & \bar{\Omega}_{22} & \bar{\Omega}_{26} \\ \bar{\Omega}_{16} & \bar{\Omega}_{26} & \bar{\Omega}_{66} \end{bmatrix} \begin{Bmatrix} \varepsilon_x \\ \varepsilon_x \\ \gamma_{xy} \end{Bmatrix} \quad \text{or} \quad \{\sigma\} = [\bar{\Omega}_{ij}]\{\varepsilon\} \qquad (i,j = 1, 2, 6) \tag{11}$$

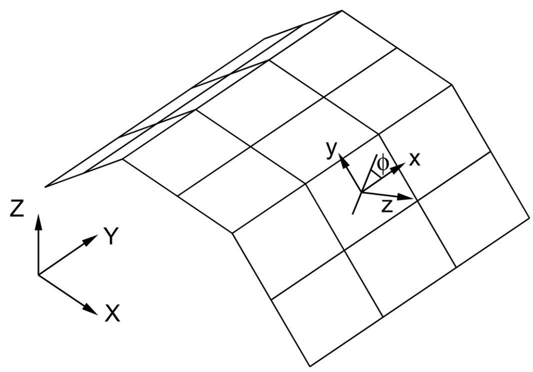

Fig. 1 Global and local axis of folded plate

$$\begin{Bmatrix} \tau_{xz} \\ \tau_{yz} \end{Bmatrix} = \begin{bmatrix} \bar{\Omega}_{44} & \bar{\Omega}_{45} \\ \bar{\Omega}_{45} & \bar{\Omega}_{55} \end{bmatrix} \begin{Bmatrix} \gamma_{xz} \\ \gamma_{yz} \end{Bmatrix} \quad \text{or} \quad \{\tau\} = [\bar{\Omega}_{ij}]\{\gamma\} \qquad (i,j = 4, 5) \tag{12}$$

$[\bar{\Omega}_{ij}]$ in Eqs. (11) and (12) is defined as

$$[\bar{\Omega}_{ij}] = [T_1]^{-1}[\Omega_{ij}][T_1]^{-T} \qquad (i,j = 1, 2, 6) \tag{13}$$

$$[\bar{\Omega}_{ij}] = [T_2]^{-1}[\Omega_{ij}][T_2] \qquad (i,j = 4, 5) \tag{14}$$

in which

$$[T_1] = \begin{bmatrix} \cos^2\phi & \sin^2\phi & 2\sin\phi\cos\phi \\ \sin^2\phi & \cos^2\phi & -2\sin\phi\cos\phi \\ -\sin\phi\cos\phi & \sin\phi\cos\phi & \cos^2\phi - \sin^2\phi \end{bmatrix} \tag{15}$$

$$[T_2] = \begin{bmatrix} \cos\phi & -\sin\phi \\ \sin\phi & \cos\phi \end{bmatrix} \tag{16}$$

$$[\Omega_{ij}] = \begin{bmatrix} \Omega_{11} & \Omega_{12} & 0 \\ \Omega_{12} & \Omega_{22} & 0 \\ 0 & 0 & \Omega_{66} \end{bmatrix} \; (i,j = 1, 2, 6), \quad [\Omega_{ij}] = \begin{bmatrix} \Omega_{44} & 0 \\ 0 & \Omega_{55} \end{bmatrix} \; (i,j = 4, 5) \tag{17}$$

$$\Omega_{11} = \frac{E_1}{1 - \nu_{12}\nu_{21}} \qquad \Omega_{12} = \frac{\nu_{12}E_2}{1 - \nu_{12}\nu_{21}} \qquad \Omega_{22} = \frac{E_2}{1 - \nu_{12}\nu_{21}} \tag{18a}$$

$$\Omega_{66} = G_{12} \qquad \Omega_{44} = G_{13} \qquad \Omega_{55} = G_{23} \tag{18b}$$

$$G_{ij} = \frac{\sqrt{E_{ij}E_{ji}}}{2(1 + \sqrt{\nu_{ij}\nu_{ji}})} \qquad (i,j = 1, 2, 3) \tag{18c}$$

The stress resultants are given by

$$\begin{bmatrix} N_x & M_x \\ N_y & M_y \\ N_{xy} & M_{xy} \end{bmatrix} = \int_{-h/2}^{h/2} \begin{bmatrix} \sigma_x \\ \sigma_y \\ \tau_{xy} \end{bmatrix} [1 \;\; z]dz \tag{19a}$$

$$\begin{bmatrix} Q_x \\ Q_y \end{bmatrix} = \int_{-h/2}^{h/2} \begin{bmatrix} \tau_{xz} \\ \tau_{yz} \end{bmatrix} dz \tag{19b}$$

From Eqs. (19a) and (19b) the constitutive equations of the folded plate are obtained as

$$\{F\} = [E]\{\chi\} \tag{20}$$

where

$$\{F\} = \{N_x, N_y, N_{xy}, M_x, M_y, M_{xy}, Q_x, Q_y\} \tag{21}$$

$$\{\chi\} = \{\varepsilon_x, \varepsilon_y, \gamma_{xy}, \kappa_x, \kappa_y, \kappa_{xy}, \gamma_{xz}, \gamma_{yz}\} \tag{22}$$

The elasticity matrix can be expressed as

$$[E] = \begin{bmatrix} [A_{ij}] & [B_{ij}] & 0 \\ [B_{ij}] & [C_{ij}] & 0 \\ 0 & 0 & [D_{ij}] \end{bmatrix} \tag{23}$$

in which

$$[A_{ij}] = \int_{-h/2}^{h/2} [\overline{\Omega}_{ij}]dz, \ [B_{ij}] = \int_{-h/2}^{h/2} [\overline{\Omega}_{ij}]zdz, \ [C_{ij}] = \int_{-h/2}^{h/2} [\overline{\Omega}_{ij}]z^2dz \quad (i, j = 1, 2, 6) \tag{24a}$$

$$[D_{ij}] = \int_{-h/2}^{h/2} [\overline{\Omega}_{ij}]dz \quad (i, j = 4, 5) \tag{24b}$$

4. The hybrid stress element

The proposed element is generated by a combination of a hybrid membrane element and a hybrid plate element.

4.1 Membrane component of the element with drilling degree of freedom

Generally membrane elements have two translational d.o.f (u, v) per node but the need for membrane elements with a drilling degree of freedom arises in many engineering problems. A drilling rotation is defined as inplane rotation about the axis normal to the plane of element. This type of element is useful in solving folded plate structures and provides an easy coupling with edge beams which have six d.o.f per node. Inclusion of a drilling degree of freedom gives also the improved behavior of the element (Allman 1984, Choi and Lee 1996). The possibility of membrane elements with drilling d.o.f was opened by Allman (1984), Bergan and Felippa (1985). The concept has been further elaborated by many other researchers (Cook 1986, MacNeal and Harder 1988, Yunus *et al.* 1989, Ibrahimbegovic *et al.* 1990, Choi and Lee 1996) for more improved elements.

Formulation of drilling d.o.f for the present element is based on the procedure given by Yunus *et al.* (1989). The displacement fields are expressed in terms of translational and rotational d.o.f.'s at the corner nodes only.

The membrane displacement field for the 4-node element is derived from an 8-node element, Fig. 2.

Rotational d.o.f. are associated with parabolic displaced shapes of element sides. In Fig. 3, rotational d.o.f. θ_{zi} and θ_{zj} are shown at nodes i and j of the element side of length L.

δ can be regarded as quadratic in side-tangent coordinates. θ_{zi} and θ_{zj} produce the edge normal displacement δ and midside value δ_m

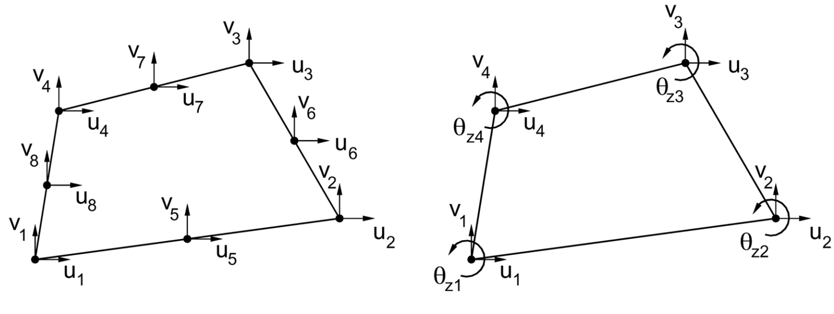

(a) (b)

Fig. 2 Displacements for (a) 8-node membrane, (b) 4-node membrane

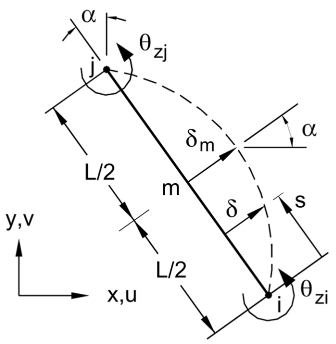

Fig. 3 Side displacement produced by drilling degrees of freedoms θ_{zi} and θ_{zj}

$$\delta = \frac{s(L-s)}{2L}(\theta_{zi} - \theta_{zj}) \qquad \delta_m = \frac{L}{8}(\theta_{zi} - \theta_{zj}) \tag{25}$$

The x and y components of δ are δ cosα and δ sinα. Therefore, after adding the contribution to displacement from nodes i and j, the total displacements u and v of a typical point on the edge are

$$\begin{Bmatrix} u \\ v \end{Bmatrix} = \frac{L-s}{L}\begin{Bmatrix} u_i \\ v_i \end{Bmatrix} + \frac{s}{L}\begin{Bmatrix} u_j \\ v_j \end{Bmatrix} + \frac{(L-s)s}{2L}(\theta_{zj} - \theta_{zi})\begin{Bmatrix} \cos\alpha \\ \sin\alpha \end{Bmatrix} \tag{26}$$

Side 1-5-2 of the element, Fig. 2 d.o.f. at node 5 are related to d.o.f. at nodes 1 and 2 of the element. By evaluating Eq. (2) with $s = L/2$ with $i = 1$, $j = 2$, $L\cos\alpha = y_2 - y_1$ and $L\sin\alpha = x_1 - x_2$, yields

$$\begin{Bmatrix} u_5 \\ v_5 \end{Bmatrix} = \frac{1}{2}\begin{Bmatrix} u_1 \\ v_1 \end{Bmatrix} + \frac{1}{2}\begin{Bmatrix} u_2 \\ v_2 \end{Bmatrix} + \frac{(\theta_{zj} - \theta_{zi})}{8}\begin{Bmatrix} y_2 - y_1 \\ x_1 - x_2 \end{Bmatrix} \tag{27}$$

After doing the same for d.o.f. at nodes 6, 7 and 8 d.o.f. in Figs. 1(b) and (c) by the transformation, the complete relation can be written

$$\{u_1 \ v_1 \ u_2 \ v_2 \ \dots \ u_8 \ v_8\}^T = [T]_{16\times 12}\{q\}^T_{membrane} \tag{28}$$

where

$$\{q\}_{membrane} = \{u_1 \;\; v_1 \;\; \theta_{z1} \;\; u_2 \;\; v_2 \;\; \theta_{z2} \;\; u_3 \;\; v_3 \;\; \theta_{z3} \;\; u_4 \;\; v_4 \;\; \theta_{z4}\} \tag{29}$$

So the midside nodal displacements can be written in terms of the corner nodal displacements and rotations and the displacement field for the 4-node, twelve d.o.f. membrane element can be derived from an 8-node membrane element. This is done through the use of the transformation matrix $[T]$. The form of $[T]$ is given in Appendix 1.

The biggest difficulty in deriving hybrid finite elements seems to be the lack of a rational methodology for deriving stress terms, Feng *et al.* (1997). It is recognized that the number of stress modes m in the assumed stress field should satisfy

$$m \geq n - r \tag{30}$$

with n the total number of nodal displacements, and r the number of rigid body modes in an element. If Eq. (30) is not satisfied, use of too few coefficients in $\{\beta\}$, the rank of the element stiffness matrix will be less than the total degrees of deformation freedom and the numerical solution of the finite element model will not be stable and produces on element with one or more mechanism.

Increasing the number of β's by adding stress modes of higher-order term, each extra term will add more stiffness and stiffens the element, Pian and Chen (1983), Punch and Atluri (1984).

The assumed stress field for the membrane part which satisfies the equilibrium conditions for zero body forces and avoid rank deficiency is given as

$$\begin{aligned} N_x &= \beta_1 + \beta_2 x + \beta_3 y + \beta_4 x^2 + \beta_5 xy + \beta_6 y^2 \\ N_y &= \beta_4 y^2 + \beta_7 + \beta_8 x + \beta_9 y + \beta_{10} x^2 + \beta_{11} xy \\ N_{xy} &= -\beta_2 y - 2\beta_4 xy - \beta_5 y^2/2 - \beta_9 x - \beta_{11} x^2/2 + \beta_{12} \end{aligned} \tag{31}$$

4.2 Plate component of the element

The flexural component of the element is identical to that of the plate bending element presented by the author, Darılmaz (2005), and corresponds to the Mindlin/Reissner plate theory. Only the assumed stress field which satisfies the equilibrium conditions for the plate part is given here.

$$\begin{aligned} M_x &= \beta_1 + \beta_4 y + \beta_6 x + \beta_8 xy \\ M_y &= \beta_2 + \beta_5 x + \beta_7 y + \beta_9 xy \\ M_{xy} &= \beta_3 + \beta_{10} x + \beta_{11} y + \beta_{12} x^2/2 + \beta_{13} y^2/2 \\ Q_x &= \beta_6 + \beta_{11} + \beta_8 y + \beta_{13} y \\ Q_y &= \beta_7 + \beta_{10} + \beta_9 x + \beta_{12} x \end{aligned} \tag{32}$$

The nodal displacements for the plate are chosen as

$$\{q\}_{plate} = \{w_1 \ \ \theta_{x1} \ \ \theta_{y1} \ \ w_2 \ \ \theta_{x2} \ \ \theta_{y2} \ \ w_3 \ \ \theta_{x3} \ \ \theta_{y3} \ \ w_4 \ \ \theta_{x4} \ \ \theta_{y4}\} \tag{33}$$

The combination of membrane and plate element yields the element which has 6 d.o.f per node and totally 24 d.o.f.

5. Element mass matrix

The problem of determination of the natural frequencies of vibration of a plate reduces to the solution of the standard eigenvalue problem $[K] - \omega^2[M] = 0$, where ω is the natural circular frequency of the system. Making use of the conventional assemblage technique of the finite element method with the necessary boundary conditions, the system matrix $[K]$ and the mass matrix $[M]$ for the entire structure can be obtained.

Element mass matrix is derived from the kinetic energy expression

$$E_k = \frac{1}{2}\int_A \{\dot{q}\}^T[R]\{\dot{q}\}dA \tag{34}$$

where $\{\dot{q}\}$ denotes the velocity components and $[R]$ is the inertia matrix.

The nodal and generalized velocity vectors are related with the help of shape functions

$$\{\dot{q}\} = \sum_{i=1}^{4}[N]\{\dot{q}_i\} \tag{35}$$

Substituting the velocity vectors in the kinetic energy, Eq. (34) yields the mass matrix of an element.

$$E_k = \frac{1}{2}\int_A \{\dot{q}_i\}^T[N]^T[R][N]\{\dot{q}_i\}dA \tag{36}$$

$$E_k = \frac{1}{2}\int_A \{\dot{q}_i\}^T[m]\{\dot{q}_i\}dA \tag{37}$$

where $[m]$ is the element consistent mass matrix and is given by

$$[m] = \int_A [N]^T[R][N]dA \tag{38}$$

6. Numerical examples

Some numerical examples have been used for assessing the accuracy of the element. The results obtained are compared with other element solutions.

Example 1:

The results of free vibration analysis of double fold cantilever folded plate are presented in Table 1

Table 1 Circular frequencies for the cantilever beam [$\varpi = \omega L\sqrt{\rho(1-\nu_{21}^2)/E_1}$]

Mode number	This study	Liu and Huang (1992)	Niyogi *et al.* (1999)	Lee and Wooh (2004)	Classical solution
1	0.1227	0.1249	0.1249	0.1211	---
2	0.1242	0.1260	0.1252	0.1348	---
3	0.2564	0.2579	0.2697	0.2561	---
4	0.2672	0.2892	0.2830	0.2869	---
5	0.3191	0.3286	0.3266	0.3253	0.329
6	0.3322	---	---	---	---

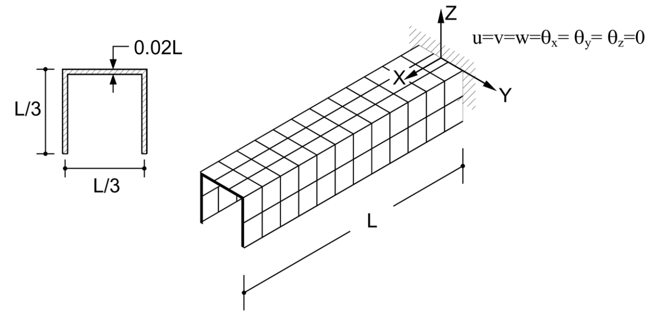

Fig. 4 The cantilever beam

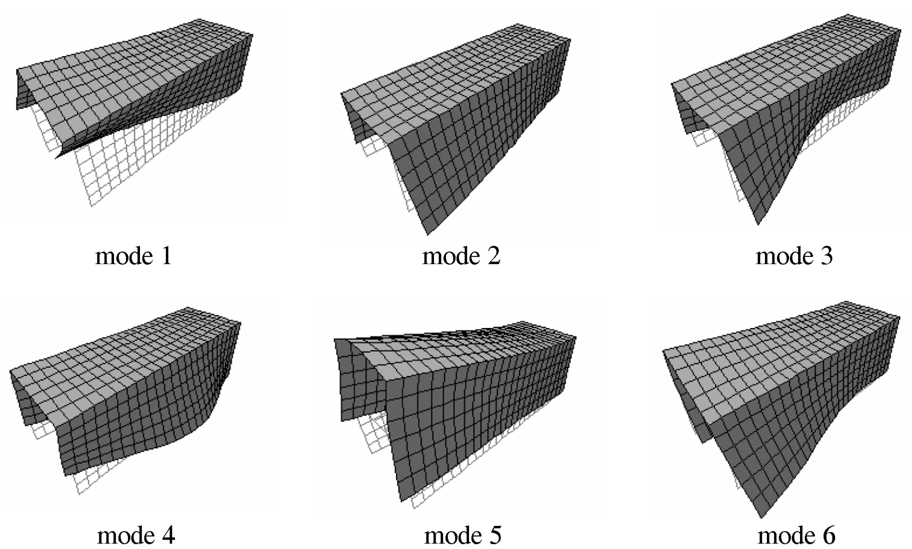

Fig. 5 First six modes of the beam

and compared with those of Liu *et al*. (1992), Niyogi *et al*. (1999) and Lee *et al*. (2004). The geometry of the folded plate is given in Fig. 4. The dimensions and material properties are chosen as $L = 2.0$ m, $t = 0.04$ m, $E_1 = 10.92 \times 10^9$ N/m^2, $\nu_{21} = 0.3$, $\rho = 1000$ kg/m^3 circular frequencies, ω, are computed for such a system.

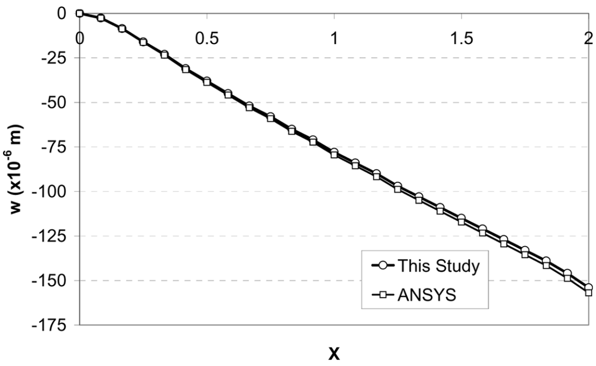

Fig. 6 Changing of w along $X(Y = 0)$

In Table 1, the first six normalized circular frequencies are given. The results are found to be in good agreement with previous works. In order to validate the element behavior a simplified solution based on beam theory is also used and results are presented as classical solution in Table 1. This simplified solution could only capture vertical vibration, mode 5.

The first six mode shapes of the beam are depicted in Fig. 5.

The system is also analysed under its self weight loading assuming weight per unit volume of material as 25 kN/m^3. In Fig. 6 the changing of w along X ($Y = 0$) is given together with ANSYS (shell63) solution. Good agreement can be obtained for static loading case.

Example 2:

A simply supported folded plate depicted in Fig. 7 is tested. The material properties used are as follows: $E_1 = 2 \times 10^7$ kN/m^2, $\nu_{21} = 0.2$, $\rho = 2500$ kg/m^3. Static analysis of the plate is carried out. The upper plate is subjected to $p = 10$ kN/m^2 uniform load.

The changing of deflection w and bending moments M_X, M_Y along A-B-C line are given in Fig. 8, Fig. 9, respectively.

The first 6 circular frequencies, ω, are computed for such a folded plate and listed in Table 2 for different cases. In order to validate the element behavior a simplified solution based on beam theory for Case A is also used and results are presented as classical solution in Table 2.

It can be observed that for obtaining the adequate accuracy in higher modes, finer meshing of the system is needed in orthotropic material case than isotropic material case.

The first six mode shapes of the system for case A are depicted in Fig. 10.

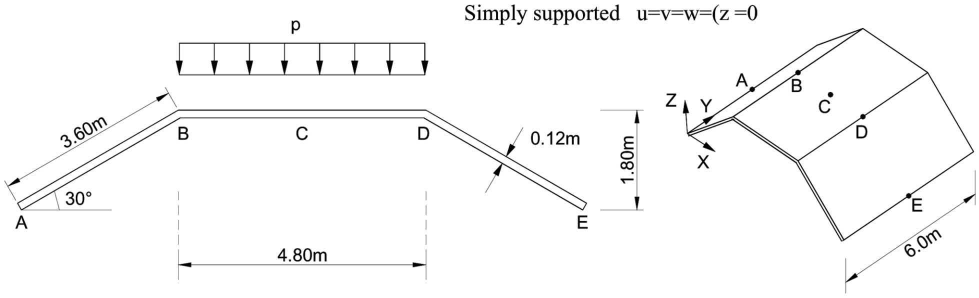

Fig. 7 Simply supported folded plate with three elements

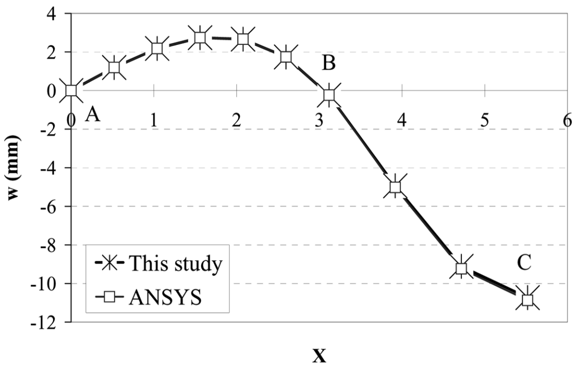

Fig. 8 Comparison of w along A-B-C line

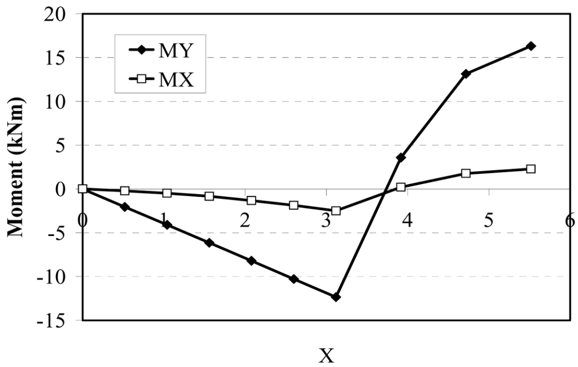

Fig. 9 M_X and M_Y moments along A-B-C line

Table 2 Circular frequencies for the folded plate with three elements

Case	E_1/E_2	ϕ	Mode number	(This study) 12 elements	(This study) 48 elements	ANSYS 12 elements	ANSYS 108 elements	Classical solution
A	1	0°	1	24.007	24.149	23.958	24.180	23.786
			2	54.686	56.065	54.338	56.149	55.325
			3	72.370	73.994	73.789	75.988	---
			4	94.075	103.047	93.544	106.807	---
			5	95.326	106.996	93.626	107.128	105.22
			6	99.135	107.983	98.935	107.499	105.79
B	10	0°	1	23.253	23.841	22.930	23.754	---
			2	46.388	55.484	35.788	55.065	---
			3	49.772	62.446	37.942	61.988	---
			4	54.213	82.22	38.697	82.592	---
			5	66.619	88.903	49.158	88.241	---
			6	75.242	105.75	71.559	104.081	---
C	10	45°	1	14.371	14.293	14.790	14.227	---
			2	34.604	34.515	34.986	34.384	---
			3	36.812	42.863	45.582	43.832	---
			4	41.489	53.848	54.925	54.689	---
			5	50.572	62.793	57.390	64.559	---
			6	52.448	67.631	60.957	68.983	---
D	10	90°	1	7.477	7.5352	7.685	7.537	---
			2	17.13	17.534	18.591	17.591	---
			3	26.026	33.429	35.108	33.611	---
			4	31.481	33.549	37.237	33.625	---
			5	34.839	34.046	37.621	34.725	---
			6	35.247	44.829	48.321	45.575	---

Results showed that the behaviour of the element is satisfactory and results are in a good agreement with other solutions.

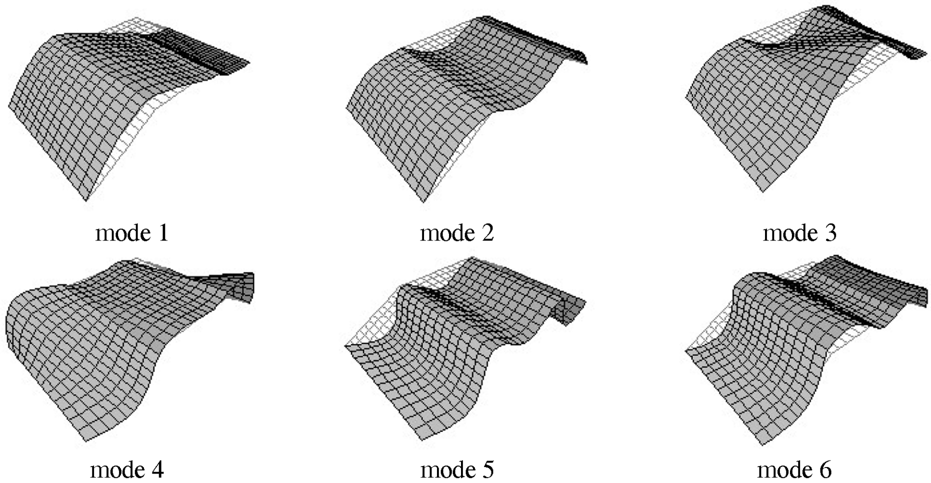

Fig. 10 First six modes of the folded plate with three elements for Case A

Example 3:

The folded plate structure investigated in this example is illustrated in Fig. 11. The dimensions of the structure are based on units of L = 10 m, the width of 10 m and thickness 0.5 m. Knife-edge loading (100 kN/m) of the center line of the upper plate is considered for static analysis. The material properties used are as, $E_1 = 2.1 \times 10^6$, $\nu_{21} = 0.3$, $\rho = 2500$ kg/m^3.

In Table 3, deflection and M_Y moment at points A and B obtained by Perry *et al.* (1992), HBHEX8R element presented by Darılmaz (2005) and ANSYS (shell63 element) are given together with the present element results for comparison.

The first six circular frequencies of the system are determined for different cases and given in Table 4.

Results obtained for both static and free vibration analysis are in a good agreement with the other element solutions. Even with the small number of elements, the present solutions have a good accuracy.

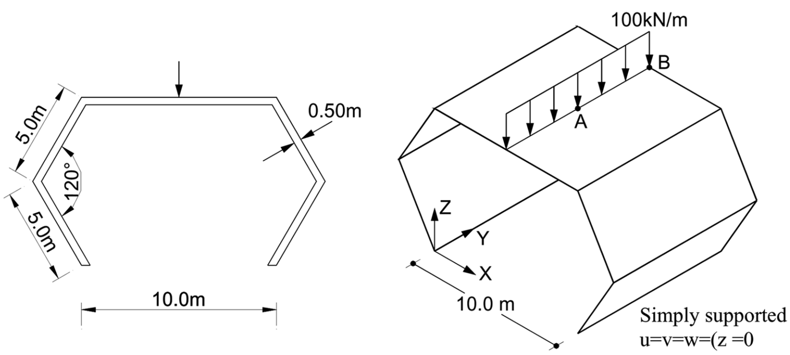

Fig. 11 Simply supported folded plate with five elements

Table 3 Comparison of w deflection and M_Y moment at points A and B

Number of elements		w_A	w_B	$M_{Y,A}$	$M_{Y,B}$
48	Perry *et al.* (1992)	0.12171	0.13101	207.2	219.6
	ANSYS	0.12180	0.12940	---	---
	Darılmaz (2005)	0.12193	0.13012	---	---
	This study	0.12133	0.12842	208.6	218.9
92	Perry *et al.* (1992)	0.12177	0.13114	207.9	220.9
	ANSYS	0.12170	0.13050	---	---
	This study	0.12163	0.13043	208.2	219.1

Table 4 Circular frequencies for the folded plate with five elements

E_1/E_2	ϕ	Mode number	This study (20 Elements)	This study (45 Elements)	ANSYS (20 Elements)	ANSYS (720 Elements)
1	0°	1	1.746	1.748	1.741	1.749
		2	8.036	8.043	8.010	8.050
		3	9.877	9.688	10.159	9.674
		4	17.281	17.308	17.156	17.323
		5	21.617	21.127	22.162	21.059
		6	30.106	30.298	29.414	30.278
10	0°	1	1.673	1.683	1.660	1.685
		2	7.308	7.180	7.263	7.294
		3	7.678	7.743	7.539	7.779
		4	16.338	16.272	15.291	16.606
		5	16.509	16.520	15.883	16.696
		6	22.555	24.631	17.653	25.123
10	45°	1	1.029	1.018	1.040	1.014
		2	4.711	4.618	4.774	4.612
		3	5.678	5.095	5.914	5.322
		4	10.162	9.675	10.391	9.743
		5	11.278	10.105	11.692	10.497
		6	18.767	16.972	18.940	17.498
10	90°	1	0.536	0.534	0.540	0.533
		2	2.476	2.460	2.492	2.463
		3	4.892	4.612	5.078	4.703
		4	5.348	5.271	5.421	5.291
		5	9.718	9.167	10.364	9.268
		6	10.269	9.490	10.724	9.678

Example 4:

Free vibration analysis of single-fold cantilever folded plate with E-glass-Epoxy composite has been carried out for the geometries shown in Fig. 12. The data used are $E_1 = 60.7 \times 10^9$ N/m^2, $E_2 = 24.8 \times 10^9$ N/m^2, $G_{12} = G_{13} = G_{23} = 12 \times 10^9$ N/m^2, $\nu_{12} = \nu_{21} = 0.23$, $\rho = 1300$ kg/m^3. In Table 5,

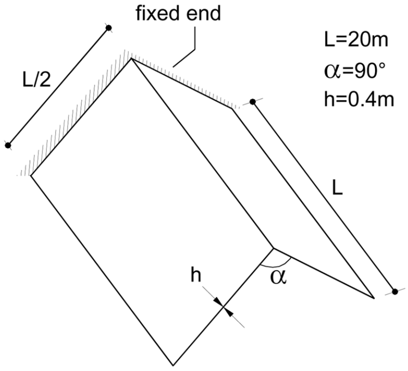

Fig. 12 Single-fold cantilever folded plate

Table 5 Non-dimensional natural frequencies for single fold composite cantilever folded plate $[\varpi = \omega L\sqrt{\rho(1-\nu_{21}^2)/E_1}]$

ϕ	Mode number	This study	Niyogi *et al.* (1999)
	1	0.0391	0.0391
0°	2	0.0677	0.0675
	3	0.1533	0.1556
	1	0.0389	0.0390
30°	2	0.0701	0.0712
	3	0.1389	0.1473
	1	0.0376	0.0381
45°	2	0.0731	0.0753
	3	0.1332	0.1406
	1	0.0359	0.0367
60°	2	0.0778	0.0804
	3	0.1295	0.1399

results compared with those of Niyogi *et al.* (1999).

Results obtained are in a good agreement with the other element solutions.

7. Conclusions

The development of an element for analysis of orthotropic folded plates was presented. The element was developed through the combination of the membrane element with a drilling degree of freedom and the Reissner-Mindlin plate bending element. Thus, the combined element element possesses six d.o.f per node, which is very conveniently used in combination with other six d.o.f per node elements for giving more accurate solutions. On the basis of the representative numerical examples, the good accuracy of the proposed element for static and free vibration analysis of folded plate structures has been demonstrated. The test results show that the element can be effectively be used for the static and free vibration analysis of folded plate structures.

Acknowledgements

The author gratefully acknowledge the excellent support and encouragement provided by Professor Dr. Nahit Kumbasar.

References

Allman, D.J. (1984), "A compatible triangular element including vertex rotations for plane elasticity problems", *Comput. Struct.*, **19**, 1-8.
ANSYS. (1997), Swanson Analysis Systems, Swanson J. ANSYS 5.4. USA.
Ayad, R., and Rigolot, A. (2002), "An improved four-node hybrid-mixed element based upon Mindlin's plate theory", *Int. J. Numer. Meth. Eng.*, **55**(6), 705-731.
Bergan, P.G. and Felippa, C.A. (1985), "A triangular membrane element with rotational degrees of freedom", *Comput. Meth. Appl. Mech. Eng.*, **50**, 25-69.
Choi, C.K. and Lee, W.H. (1996), "Versatile variable-node flat-shell element", *J. Eng. Mech*., **122**(5), 432-441.
Cook, R.D. (1986), "On the Allman triangle and a related quadrilateral element", *Comput. Struct.*, **22**, 1065-1067.
Ibrahimbegovic, A., Taylor, R.L. and Wison, E.L. (1990), "A robust quadrilateral membrane finite element with drilling degrees of freedom", *Int. J. Numer. Meth. Eng.*, **30**, 445-457.
Darılmaz, K. (2005), "An assumed-stress finite element for static and free vibration analysis of Reissner-Mindlin plates", *Struct. Eng. Mech.*, **19**(2), 199-215.
Darılmaz, K. (2005), "A hybrid 8-node hexahedral element for static and free vibration analysis", *Struct. Eng. Mech.*, **21**(5), 571-590.
Duan, M. and Miyamoto, Y. (2002), "Effective hybrid/mixed finite elements for folded-plate structures", *J. Eng. Mech.,* ASCE, **128**(2), 202-208.
Eratli, N. and Akoz, A.Y. (2002), "Mixed finite element formulation for folded plates", *Struct. Eng. Mech.*, **13**(2), 155-170.
Feng, W., Hoa, S.V. and Huang, Q. (1997), "Classification of stress modes in assumed stress fields of hybrid finite elements", *Int. J. Numer. Meth. Eng*., **40**, 4313-4339.
Lee, S.Y. and Wooh, S.C. (2004) "Finite element vibration analysis of composite box structures using the high order plate theory", *J. Sound Vib.,* **277**(4-5), 801-814.
Liu, W.H. and Huang, C.C. (1992), "Vibration Analysis of folded plates", *J. Sound Vib.*, **157**, 123-137.
MacNeal, R.H. and Harder, R.L. (1988), "A refined four-noded membrane element with rotational degrees of freedom", *Comput. Struct.*, **28**, 75-84.
Niyogi, A.G., Laha, M.K. and Sinha, P.K. (1999), "Finite element vibration analysis of laminated composite folded plate structures", *Shock and Vibration*, **6**, 273-283.
Perry, B., Bar-Yoseph, P. and Rosenhouse, G. (1992), "Rectangular hybrid shell element for analysing folded plate structures", *Comput. Struct.*, **44**, 177-183.
Pian, T.H.H. (1964), "Derivation of element stiffness matrices by assumed stress distributions", *AIAA J.*, **12**, 1333-1336.
Pian, T.H.H. and Chen, D.P. (1983), "On the suppression of zero energy deformation modes", *Int. J. Numer. Meth. Eng*., **19**, 1741-1752.
Punch, E.F. and Atluri, S.N. (1984), "Development and testing of stable, isoparametric curvilinear 2 and 3-D hybrid stress elements", *Comput. Meth. Appl. Mech. Eng*., **47**, 331-356.
Yunus, S.M., Saigal, S. and Cook, R.D. (1989), "On improved hybrid finite elements with rotational degrees of freedom", *Int. J. Numer. Meth. Eng.*, **28**, 785-800.

Appendix 1:

$$[T] = \begin{bmatrix}
1 & 0 & 0 & 0 & 0 & 0 & 0 & 0 & 0 & 0 & 0 & 0 \\
0 & 1 & 0 & 0 & 0 & 0 & 0 & 0 & 0 & 0 & 0 & 0 \\
0 & 0 & 0 & 1 & 0 & 0 & 0 & 0 & 0 & 0 & 0 & 0 \\
0 & 0 & 0 & 0 & 1 & 0 & 0 & 0 & 0 & 0 & 0 & 0 \\
0 & 0 & 0 & 0 & 0 & 0 & 1 & 0 & 0 & 0 & 0 & 0 \\
0 & 0 & 0 & 0 & 0 & 0 & 0 & 1 & 0 & 0 & 0 & 0 \\
0 & 0 & 0 & 0 & 0 & 0 & 0 & 0 & 0 & 1 & 0 & 0 \\
0 & 0 & 0 & 0 & 0 & 0 & 0 & 0 & 0 & 0 & 1 & 0 \\
\frac{1}{2} & 0 & \frac{(y_1-y_2)}{8} & \frac{1}{2} & 0 & \frac{(y_2-y_1)}{8} & 0 & 0 & 0 & 0 & 0 & 0 \\
0 & \frac{1}{2} & \frac{(x_2-x_1)}{8} & 0 & \frac{1}{2} & \frac{(x_1-x_2)}{8} & 0 & 0 & 0 & 0 & 0 & 0 \\
0 & 0 & 0 & \frac{1}{2} & 0 & \frac{(y_2-y_3)}{8} & \frac{1}{2} & 0 & \frac{(y_3-y_2)}{8} & 0 & 0 & 0 \\
0 & 0 & 0 & 0 & \frac{1}{2} & \frac{(x_3-x_2)}{8} & 0 & \frac{1}{2} & \frac{(x_2-x_3)}{8} & 0 & 0 & 0 \\
0 & 0 & 0 & 0 & 0 & 0 & \frac{1}{2} & 0 & \frac{(y_3-y_4)}{8} & \frac{1}{2} & 0 & \frac{(y_4-y_3)}{8} \\
0 & 0 & 0 & 0 & 0 & 0 & 0 & \frac{1}{2} & \frac{(x_4-x_3)}{8} & 0 & \frac{1}{2} & \frac{(x_3-x_4)}{8} \\
\frac{1}{2} & 0 & \frac{(y_1-y_4)}{8} & 0 & 0 & 0 & 0 & 0 & 0 & \frac{1}{2} & 0 & \frac{(y_4-y_1)}{8} \\
0 & \frac{1}{2} & \frac{(x_4-x_1)}{8} & 0 & 0 & 0 & 0 & 0 & 0 & 0 & \frac{1}{2} & \frac{(x_1-x_4)}{8}
\end{bmatrix}$$

Appendix 2:
Notation

E_1, E_2	: moduli of elasticity along x and y axes of element respectively
G_{12}, G_{13}, G_{23}	: shear moduli of elasticity in x-y, x-z and y-z planes of element
x, y, z	: element local axis
X, Y, Z	: system global axis
ν_{12}, ν_{21}	: Poisson ratio
$[D]$	: differential operator matrix
$[E]$	: elasticity matrix
$[G]$	: nodal forces corresponding to assumed stress field
$[N]$	: shape functions
$[R]$	: inertia matrix
$[P]$	: interpolation matrix for stress
$\{q\}$, $\{\dot{q}\}$	: displacement and velocity components
$\{u\}$	: displacements
$\{\beta\}$	: stress parameters
$\{\sigma\}$	: internal forces

Q_x, Q_y	: internal shear forces per unit length
N_x, N_y, N_y	: membrane forces per unit length
M_x, M_y, M_{xy}	: internal moments per unit length
ρ	: mass per unit volume
ω	: natural circular frequency
ϕ	: material angle in an element with reference to x-axis